



NJC

**Adsorption of Solid Phosphines on Silica and Implications  
for  
Catalysts on Oxide Surfaces**

Journal:	<i>New Journal of Chemistry</i>
Manuscript ID	NJ-ART-06-2023-003016.R1
Article Type:	Paper
Date Submitted by the Author:	21-Oct-2023
Complete List of Authors:	Hoefler, John; Texas A&M University, Department of Chemistry Yang, Yuan; Colorado School of Mines, Chemistry Bluemel, Janet; Texas A&M University, Department of Chemistry

SCHOLARONE™  
Manuscripts

# Adsorption of Solid Phosphines on Silica and Implications for Catalysts on Oxide Surfaces

John C. Hoefler<sup>#</sup>, Yuan Yang<sup>†,\*</sup>, Janet Blümel<sup>#,\*</sup>

<sup>#</sup>Department of Chemistry, Texas A&M University, College Station, Texas, United States

<sup>†</sup>Department of Chemistry, Colorado School of Mines, Golden, Colorado, United States

**ABSTRACT:** Tertiary phosphines are ubiquitous in inorganic chemistry. They play important roles as ligands in coordination chemistry and catalysis. Furthermore, they act as surface acidity probes for oxide surfaces. However, only volatile phosphines, such as  $\text{PH}_3$  have been applied in this function so far. Here we demonstrate for the first time that the triaryl- and trialkylphosphines  $\text{PPh}_3$  and  $\text{PCy}_3$  with high melting points self-adsorb readily onto a silica surface even in the absence of a solvent. The self-adsorption takes place within days when both solid components are mixed and then left undisturbed. The phosphines form well-defined monolayers on the surface and the transition from monolayer to left-over polycrystalline phosphine is abrupt. Therefore, the maximal surface coverage with a monolayer can be easily determined. When the phosphines are adsorbed from solutions, the same maximal surface coverage is found. Solid-state NMR spectroscopy provides a unique analytical tool for studying the structure and dynamics of phosphines in different environments.  $^{31}\text{P}$  and  $^2\text{H}$  solid-state NMR measurements are successfully applied for characterizing the adsorption process and the mobilities of the adsorbed phosphines across the silica surface. Furthermore, using  $(\text{Ph}_3\text{P})_2\text{Ni}(\text{CO})_2$  as a representative, it is demonstrated that the silica surface has a hitherto unrecognized impact on immobilized and surface-residing catalysts because it competes for phosphine ligands coordinated to a metal center. This competition manifests as one more factor leading to the loss of phosphine ligands and ultimately leaching of immobilized metal complexes or nanoparticle formation. Besides the increase of fundamental knowledge about adsorption processes, the presented results have implications for chromatographic separations of metal complexes and for the lifetime of immobilized and other types of surface-residing catalysts.

## INTRODUCTION

The adsorption of molecules on a surface is ubiquitous in academia and industry and is applied for numerous analytical and purification purposes.<sup>1</sup> In contrast to chemical bonding or immobilization,<sup>2-4</sup> the term physical adsorption is associated with a process where no electrons are transferred between the adsorbed molecules and the adsorbent surface.<sup>1</sup> The interaction is caused mainly by van der Waals forces, and the adsorption is fully reversible. For example, volatile compounds are removed from a surface *in vacuo*. Alternatively, a non-volatile adsorbate can be washed off with a favorable solvent.

Although adsorption is often disregarded when working with covalently bound species on a surface, it does have an impact on many systems and hitherto unrecognized implications. For example, immobilized catalysts<sup>2-5</sup> are impacted by adsorption of ligands on support surfaces. The competition between the metal center and the surface for the coordinated phosphine can lead to a loss of the ligands and leaching of the metal from the surface as demonstrated in the results and discussion section.

Neutral silica<sup>6</sup> is the prevalent support for adsorption studies because of its mechanical stability during grinding, comparatively unreactive nature, and relatively large surface area of  $750 \text{ m}^2/\text{g}$ . From a practical perspective, it easily packs into a solid-state NMR

rotor and due to its large average particle diameters (0.062-0.2 mm) it can be handled in a glove-box or at the Schlenk line under an inert gas stream without dust issues. The adsorption results obtained with a silica surface for metallocenes<sup>7-10</sup> and phosphine oxides<sup>11,12</sup> translate to other surfaces such as alumina or activated carbon, as demonstrated in the case of ferrocene adsorbed on activated carbon<sup>13,14</sup> and triphenylphosphine oxide adsorbed on alumina.<sup>15</sup>

We and others have previously shown that diverse species with high melting points can be adsorbed on solid supports in the absence of solvents. For example, solid metallocenes,<sup>7-10</sup> phosphine oxides,<sup>11,12,15</sup> and polycyclic aromatic hydrocarbons (PAH)<sup>16</sup> including their chromium tricarbonyl complexes,<sup>17</sup> can be adsorbed on a variety of surfaces by grinding the dry components with a mortar and pestle or just bringing the solid components into contact.<sup>8,10</sup> The nucleus  $^{31}\text{P}$  is ideal to probe the dynamics and structures of surface-bound species containing phosphorus<sup>11,12,15,18</sup> by solid-state NMR spectroscopy.<sup>19-24</sup>

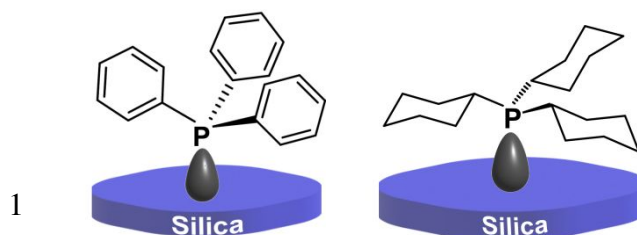


**Figure 1.** Schematic display of PPh<sub>3</sub> (**1**) and PCy<sub>3</sub> (**2**) adsorbed on a silica surface as **1a** and **2a**.

Phosphines and their adsorption are important, for example, in the field of nanoparticle catalysis, where phosphine capping ligands can be used to tune properties such as the nanoparticle size.<sup>25</sup> For adsorption on support surfaces phosphines like PH<sub>3</sub><sup>26-28</sup> and allyldiphenylphosphine<sup>29</sup> have been used. For probing the Brønsted-acidic sites of sulfated zirconium oxide, diverse sterically hindered tertiary phosphines, including PPh<sub>3</sub>, have been applied.<sup>30</sup> For this strongly acidic surface it could be demonstrated that phosphonium salts of the type R<sub>3</sub>PH<sup>+</sup> are generated.<sup>30</sup> The silica surfaces used in this contribution are much less acidic and lack the potential to protonate even the more basic alkyl diaryl phosphines, as proven by dipolar dephasing methods earlier.<sup>31</sup>

Interestingly, solid phosphines with high melting points, such as PPh<sub>3</sub> (80 °C) and PCy<sub>3</sub> (82 °C) have rarely been considered for adsorption studies (Figure 1).<sup>30</sup> The interaction of phosphines with a silica surface is expected to be weaker than for phosphine oxides,<sup>11,12,15</sup> as no hydrogen bonds between P=O groups and surface OH groups can form. Therefore, it is interesting to probe whether weak van der Waals interactions with a neutral silica surface suffice to overcome the lattice energy of solid phosphines. Furthermore, the moiety of PPh<sub>3</sub> actually interacting with the surface has to be identified. It could be one of the phenyl groups or the lone pair at the phosphorus atom. Finally, gaining insight into the mobilities of the phosphine molecules on the surface and probing the impact of phosphine adsorption on metal complexes with phosphine ligands that come into contact with silica was also investigated.

In this contribution, we demonstrate that the high-melting phosphines PPh<sub>3</sub> (**1**) and PCy<sub>3</sub> (**2**) can be adsorbed on a silica surface as **1a** and **2a** not only from a solution, but also by dry grinding of the components in the absence of a solvent (Figure 1). The progress of the dry adsorption is monitored by <sup>31</sup>P solid-state NMR. The averaging out of anisotropic interactions and T<sub>1</sub> relaxation time measurements confirm the change from polycrystalline **1** to surface-adsorbed **1a** and **2a**. Selectively deuterated PPh<sub>3</sub>-d<sub>1</sub> (Ph<sub>2</sub>P(*p*-C<sub>6</sub>H<sub>4</sub>D), **1-d**<sub>1</sub>), PPh<sub>3</sub>-d<sub>3</sub> (P(*p*-C<sub>6</sub>H<sub>4</sub>D)<sub>3</sub>, **1-d**<sub>3</sub>), and PPh<sub>3</sub>-d<sub>5</sub> (Ph<sub>2</sub>P(C<sub>6</sub>D<sub>5</sub>), **1-d**<sub>5</sub>) allowed the additional use of <sup>2</sup>H solid-state NMR spectroscopy to confirm the rapid motion of the adsorbed phosphine molecules across the silica surface at ambient temperature. Experiments applying the phosphine nickel complex (Ph<sub>3</sub>P)<sub>2</sub>Ni(CO)<sub>2</sub> to the surface show that silica competes for the phosphine ligands and removes them from the metal center.

## RESULTS AND DISCUSSION

Polycrystalline PPh<sub>3</sub> (**1**) is a solid with a high melting point of 80 °C. Its <sup>31</sup>P CP/MAS spectra, recorded at different spinning speeds, exhibit a narrow isotropic line at δ<sub>iso</sub> = -9.4 ppm with a halfwidth of about 70 Hz. The chemical shift is in accordance with the values reported in the literature (-7 ppm,<sup>21</sup> -8 ppm,<sup>32</sup> and -10 ppm<sup>21</sup>) (Figure S1). The rotational sidebands indicate a CSA (chemical shift anisotropy) pattern<sup>20,21</sup> that manifests in the wide-line spectrum recorded without sample spinning. The CSA

parameters are δ<sub>11</sub> (7 ppm), δ<sub>22</sub> (7 ppm) and δ<sub>33</sub> (-43 ppm) with a span<sup>21</sup> of 51 ppm. The appearance of the 4 kHz spectrum changes drastically when **1** is adsorbed on silica from a diethyl ether solution to form **1a** (Figure 2). After complete removal of the solvent, the CSA is reduced to the point where no rotational sidebands are visible any longer. This translates to averaging of chemical shift anisotropy due to fast motion of the adsorbed molecules. They are reorienting fast and quasi-isotropically by spiraling movements on the surface within the pores of the silica.

In fact, the molecules of **1a**, adsorbed in a sub-monolayer coverage (20 mg per g of silica, 7 molecules per 100 nm<sup>2</sup>) are so mobile on the silica surface that the residual linewidth of the <sup>31</sup>P CP/MAS signal does not increase substantially when the spinning speed is lowered from 4 kHz (linewidth 420 Hz) to 2 kHz (550 Hz). Even when the sample is not spun at all, the residual linewidth of the signal remains comparatively small (920 Hz). As detailed below, the residual halfwidths are also dependent on the surface coverage. However, regarding one specific surface coverage, the minimal impact of sample spinning on the halfwidth persists. For example, a monolayer coverage with **1a** (206 molecules on 100 nm<sup>2</sup>) shows the same trend. The halfwidth of the <sup>31</sup>P CP/MAS signal is 340 Hz at 4 kHz spinning speed and only slightly larger without sample rotation (520 Hz) (Figure S2). Higher rotational frequencies do not further reduce the residual linewidths in the CP/MAS spectra.

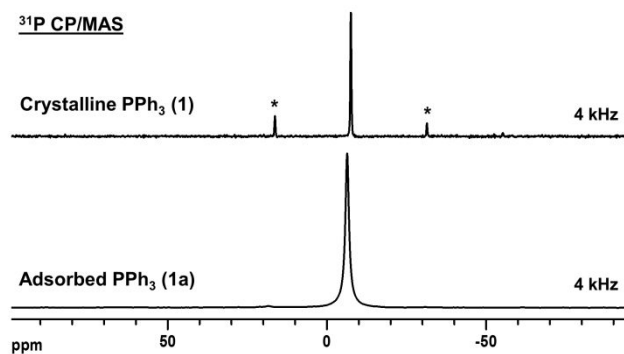


**Figure 2.** <sup>31</sup>P CP/MAS spectra of PPh<sub>3</sub> (**1**) (top), and PPh<sub>3</sub> adsorbed on silica (**1a**, 0.1 g on 1 g of silica) (bottom). Asterisks denote rotational sidebands.

Finally, the adsorption also manifests in a downfield shift of the <sup>31</sup>P NMR signal from -10 ppm to -6 ppm. This indicates that the free electron pair at phosphorus is interacting with either surface silanol or siloxane groups.<sup>33</sup> Although, in contrast to triphenylphosphine oxide, no hydrogen bond in the classical sense can form, the electron withdrawing effect of the surface on the phosphorus nucleus is noticeable. The influence of the surface properties of silica on the line shape is investigated below.

In principle, the line-narrowing and CSA-reducing effects seen in the <sup>31</sup>P CP/MAS spectra of **1a** could stem from partial quaternization at the phosphorus. For example, it has been demonstrated earlier that the quaternary phosphonium cations [R<sub>3</sub>EtP]<sup>+</sup> exhibit much smaller CSA values than phosphine oxides due to the higher electronic symmetry at the <sup>31</sup>P nucleus.<sup>34</sup>

Therefore, in order to ascertain that the molecules of **1a** are translationally mobile, the  $^{13}\text{C}$  CP/MAS spectra of **1** and **1a** have been recorded (Figure 3). A sample of polycrystalline **1** gives overlapping aromatic carbon signals of the phenyl groups with the characteristically large CSA.<sup>21</sup> After adsorption as **1a**, the rotational sidebands vanish and the isotropic aryl signals are nearly resolved (Figure 3). This indicates that the phenyl groups in **1** are mobile, too, since quaternization at phosphorus alone would not change the CSA of the aryl carbons.

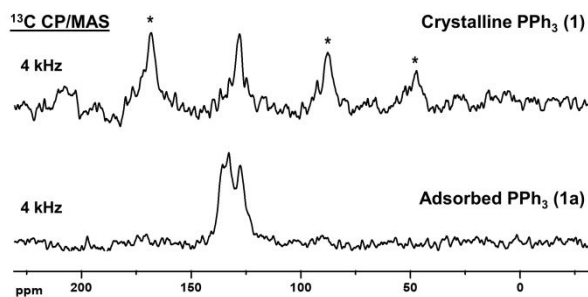


**Figure 3.**  $^{13}\text{C}$  CP/MAS spectra of polycrystalline  $\text{PPh}_3$  (**1**, top) and surface-adsorbed  $\text{PPh}_3$  (**1a**, bottom) at 4 kHz spinning speed. The contact time for all measurements was 5 ms. Asterisks denote rotational sidebands.

Based on the geometry of **1**, derived from the X-ray structure of  $\text{PPh}_3$ ,<sup>35</sup> the phenyl groups cannot interact with the silica surface by aligning parallel to it like benzene<sup>36,37</sup> without participation of the free electron pair at phosphorus. Nevertheless, some crucial interaction of the aromatic rings with the surface could occur, as the research on adsorbed PAH shows.<sup>16,17</sup> In order to exclude the interaction of the aromatic system with the surface as the driving force behind the adsorption,  $\text{PCy}_3$  (**2**) has been administered on the surface to yield **2a** as described for **1a** above. The  $^{31}\text{P}$  CP/MAS spectra of polycrystalline **2** show the expected large CSA with a span<sup>21</sup> of 65 ppm and the parameters  $\delta_{11}$  (36 ppm),  $\delta_{22}$  (13 ppm), and  $\delta_{33}$  (-29 ppm), in accordance with reported values<sup>21</sup> (Figure 4) and a narrow isotropic line with a halfwidth of 110 Hz at 7 ppm. However, after adsorption, **2a** yields a broadened isotropic line featuring a halfwidth of 600 Hz, but no more rotational sidebands. The drastically reduced CSA of **2a** proves that the adsorption phenomenon also takes place when a solid trialkylphosphine with a high melting point is used and that it is independent of the presence of aromatic substituents at phosphorus. Therefore, it can be concluded that the adsorption is mainly driven by the lone pair at the phosphorus atom interacting with the surface.

Tertiary phosphines adsorb on the silica surface readily when applied from a solution. Interestingly, the adsorption process also takes place when the dry components are brought into contact. After manually grinding  $\text{PPh}_3$  and silica together with a mortar and pestle for an hour and then placing the mixture in a rotor, the solvent-free adsorption process can be monitored with  $^{31}\text{P}$  CP/MAS (Figure 5). Adsorbed **1a** is already visible after one hour with a signal downfield-shifted from that of polycrystalline **1**. The dry self-adsorption then progresses without further handling of the

mixture over the course of 17 days.

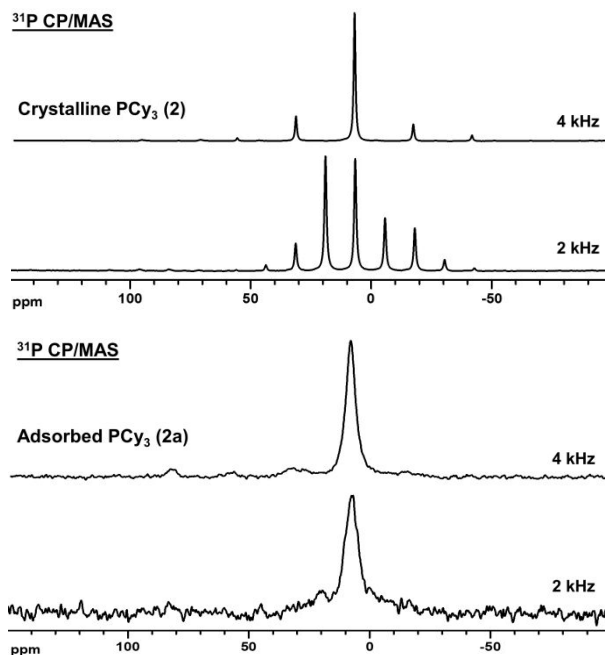


**Figure 4.**  $^{31}\text{P}$  CP/MAS spectra of polycrystalline  $\text{PCy}_3$  (**2**) (top two spectra), and  $\text{PCy}_3$  adsorbed on silica (**2a**) (bottom two spectra) at the indicated rotational speeds.

Although the adsorption without solvent takes much longer than applying **1** from solution, it offers important insights. In general, the solvent-free adsorption presents an example illustrating that solids are not inert and react or interact with each other over time even in the absence of solvents. This is a key factor enabling mechanochemistry that typically applies higher temperatures and pressures to speed up the solvent-free reactions. Only one example of isostructural solid metallocenes forming solid solutions at ambient temperatures has been described.<sup>38</sup>

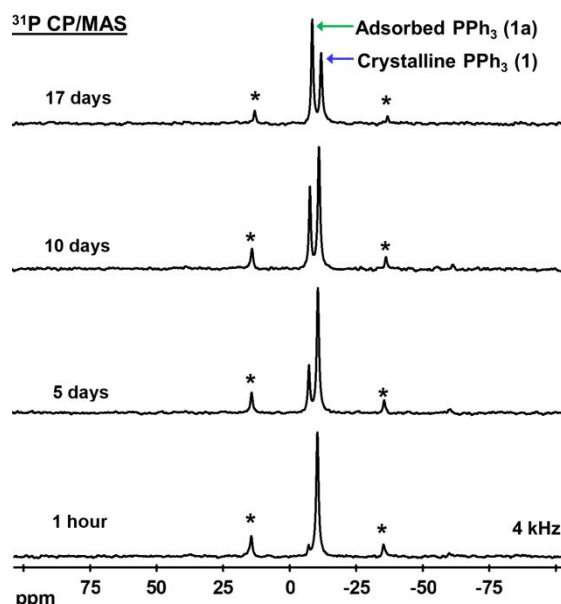


**Figure 5.**  $^{31}\text{P}$  CP/MAS spectra of polycrystalline  $\text{PPh}_3$  (**1**), slowly being adsorbed on silica in the absence of a solvent to form **1a**, recorded at the given intervals. Asterisks denote rotational sidebands of residual **1**.

Furthermore, regarding the adsorption of **1**, the sequence of spectra displayed in Figure 5 shows that the transition from polycrystalline to adsorbed molecules is abrupt. Once a monolayer of **1a** on the surface is complete, excess polycrystalline **1** is left over. There is no gradual merging of the signals of **1** and **1a**. This becomes even more obvious when a sample with partially adsorbed  $\text{PPh}_3$  is measured with  $^{31}\text{P}$  CP while spinning slowly at 2 kHz and recording the spectrum without sample rotation (Figure 6). The polycrystalline component **1** results in the characteristic CSA pattern, while the narrow signal of **1a** resides on top of it. The nicely separated signals of adsorbed and polycrystalline material allow for the determination of the maximal surface coverage once the ratio of **1** to **1a** remains constant. For the silica used for this experiment the maximal monolayer surface coverage amounts to 3.076 g of **1a** per 1 g of silica, corresponding to about 206 molecules per 100 nm<sup>2</sup> of surface area. Importantly, the maximal monolayer surface coverage is the same when **1** is adsorbed by applying a solution and subsequently removing the solvent *in vacuo*.

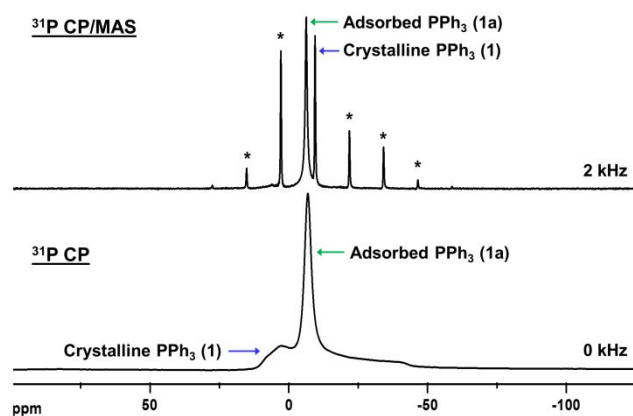


**Figure 6.**  $^{31}\text{P}$  CP/MAS spectra of  $\text{PPh}_3$  adsorbed on silica (**1a**) and residual polycrystalline **1** after dry-grinding and aging for 17 days. Asterisks denote rotational sidebands of residual **1**.

As an additional proof that polycrystalline **1** assumes a different physical state when adsorbed on the silica surface, the  $^{31}\text{P}$   $T_1$  relaxation times of **1** and **1a**, obtained by inversion recovery techniques,<sup>19,38</sup> were compared. While the  $T_1$  time of polycrystalline **1** is about 1000 s,<sup>32</sup> it is merely 0.59 s when 0.1 g of the phosphine is adsorbed on 1 g of silica (Figures S3, Figure S4, Table S1). The more than three orders of magnitude smaller value for **1a** indicates the much higher mobility of the  $\text{PPh}_3$  molecules on the surface. The  $T_1$  relaxation time does not increase substantially, when the surface coverage is increased fourfold. For example, 0.4 g of **1a** on the surface of 1 g of silica leads to a value of 0.63 s (Figure S4). This means that the mobility remains high when quadrupling the surface coverage from about 34 molecules to 134 molecules of **1a** per nm<sup>2</sup>. This observation is corroborated by

the dependence of the residual linewidths of the  $^{31}\text{P}$  CP/MAS signal of **1a** on the surface coverage. The linewidth decreases with increasing surface coverage in the low coverage region (Figure S5). An example has been discussed above. This linewidth dependence is in accordance with earlier observations on covalently bound phosphines.<sup>2</sup>

Another related indicator of mobility is the CP contact time dependence. As expected for an immobile molecule residing within a crystal lattice and containing only aryl protons, for polycrystalline  $\text{PPh}_3$  longer contact times lead to increased signal intensities (Figure S6).<sup>39</sup> On the other hand, for the mobile molecules in **1a** a shorter contact time of about 3 ms results in optimal signal intensity, while longer contact times lead to deteriorated S/N ratios (Figure S6). The proton-rich  $\text{PCy}_3$  follows the same trend. The  $^{31}\text{P}$  CP/MAS signal of polycrystalline **2** profits from longer contact times. In contrast, **2a** requires a short contact time of 0.5 ms for optimal S/N ratios (Figure S6).<sup>12,33,39</sup>

Besides the CSA, heteronuclear dipolar interactions between the protons and the  $^{31}\text{P}$  nucleus lead to a broadening of its signal. In the CP/MAS spectra discussed above, the  $^1\text{H}/^{31}\text{P}$  heteronuclear dipolar interactions had been eliminated by high-power proton decoupling (Figure 2, Figure S2). When polycrystalline **1** is probed by  $^{31}\text{P}$  MAS using a single pulse program without proton decoupling, the residual linewidth of the signal (1.4 kHz) is large even at 4 kHz rotational frequency, while the CSA is still visible via the first order rotational sidebands (Figure S7). In contrast, even without high-power proton decoupling the resonance of **1a** is rather narrow (420 Hz) and decoupling only leads to a moderate decrease of the residual linewidth to 360 Hz. This demonstrates that heteronuclear dipolar interactions are efficiently eliminated already by the mobility of the molecules of **1a** on the surface. This becomes even more obvious when considering the wide-line  $^{31}\text{P}$  spectra of polycrystalline **1** and adsorbed **1a** (Figure S8). Without rotation and proton decoupling the signal of **1** is broad and unstructured, spanning about 7.2 kHz. Under the same measurement conditions a narrow signal is obtained for **1a** (460 Hz halfwidth). Interestingly, proton decoupling broadens the signal to 1 kHz, most probably due to interference of the decoupling frequency with the reorientation of the molecules on the surface within the pores. This broadening effect due to decoupling has been described earlier involving the ring rotation in decamethylchromocene.<sup>40</sup>

Quadrupolar interactions lead to large signals with characteristic patterns for quadrupolar nuclei in the solid state. These patterns can be used for analytical purposes. For example, the Pake pattern of deuterium nuclei has been used widely for probing mobile species and moieties in the solid state.<sup>13,22,41,42</sup> Therefore, we synthesized three deuterated versions of **1**,  $\text{PPh}_3\text{-}d_1$  ( $\text{Ph}_2\text{P}(p\text{-C}_6\text{H}_4\text{D})$ , **1-}d\_1),  $\text{PPh}_3\text{-}d_3$  ( $\text{P}(p\text{-C}_6\text{H}_4\text{D})_3$ , **1-}d\_3), and  $\text{PPh}_3\text{-}d_5$  ( $\text{Ph}_2\text{P}(\text{C}_6\text{D}_5)$ , **1-}d\_5).******

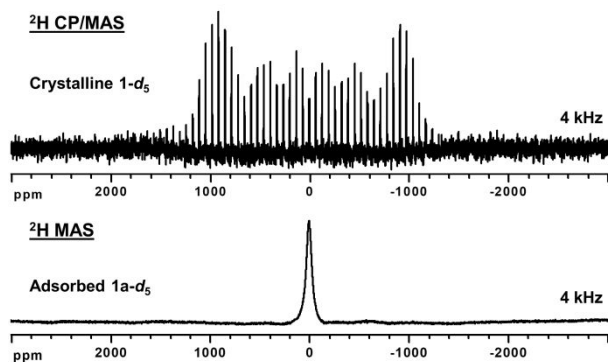


**Figure 7.**  $^2\text{H}$  CP/MAS spectrum of polycrystalline  $1\text{-}d_5$  (top) and MAS spectrum of surface-adsorbed  $1\text{a-}d_5$  (bottom) at 4 kHz spinning speed.

All  $^2\text{H}$  CP/MAS spectra of the polycrystalline deuterated phosphines show Pake patterns (Figure 7, Figure S9) with the quadrupolar coupling constants  $Q_{\text{CC}}$  160 kHz ( $1\text{-}d_1$ ) and 149 kHz ( $1\text{-}d_3$ ,  $1\text{-}d_5$ ). However, once adsorbed on silica the large quadrupolar interactions are averaged out due to the translational mobility of the molecules of  $1\text{a-}d_1$ ,  $1\text{a-}d_3$ , and  $1\text{a-}d_5$  on the curved surface and only the relatively narrow isotropic lines remain. Comparing the linewidths (1.5, 6.4, and 5.0 kHz) and appearances of the signals with calculated lineshapes<sup>41</sup> shows that the maximal reorientation time corresponds to about 0.3  $\mu\text{s}$ . It is noteworthy that the adsorbed phosphines do not show signals when measured with cross polarization due to their mobility.<sup>43</sup>

Next, we performed preliminary studies about how the nature of the silica surface<sup>6,43</sup> and its pore size influence the mobility of  $1\text{a}$ . For the latter, the same amount of  $1$  was adsorbed on silica batches with average pore diameters of 40 and 100 Å. Both the chemical shifts ( $-6$  ppm) and linewidths (230 and 200 Hz) of the  $^{31}\text{P}$  CP/MAS signals were in the same range, indicating that the pore size does not have a major impact on the mobility of the molecules of  $1\text{a}$  on the surface (Figure S10, Table S2). For probing whether the number of silanol groups on the surface makes a difference, the same amount of  $1$  was added to batches of silica rigorously dried *in vacuo* at 600 °C and "wet" silica that had been dried at ambient temperature to just remove the adsorbed water.<sup>6,43</sup> The  $^{31}\text{P}$  CP/MAS spectra again do not show any difference (Figure S11). The chemical shifts and linewidths are identical ( $-6$  ppm, 230 Hz). Therefore, it can be concluded that the polarity of the surface does not play a crucial role and that the driving force of the adsorption is van der Waals interactions rather than specific interactions with surface silanol groups.

Finally,  $\text{Me}_3\text{Si}$ -modified silica, generated by reacting silica with neat  $\text{Me}_3\text{OEt}$ ,<sup>43</sup> has been applied to probe whether rendering the surface hydrophobic and implementing mechanical obstacles for the mobile molecules of  $1\text{a}$  would make a difference. As the  $^{31}\text{P}$  CP/MAS spectrum shows, the adsorption takes place and the  $\text{PPh}_3$  molecules are highly mobile across this modified surface as well (Figure S12). The signal halfwidth amounts to 200 Hz and is within the typical range, as is the chemical shift with  $-6$  ppm. This result is another indicator that hydrogen bonding to silanol groups does not play a major role in the adsorption of  $1$  on silica. Furthermore, the  $\text{Me}_3\text{Si}$  groups do not present obstacles that would slow down the adsorbed molecules of  $1\text{a}$ .

The adsorption of phosphines on silica surfaces is phenomenologically important. It also has implications for phosphines coordinated in metal complexes. In case the phosphines serve as linkers for immobilized catalysts,<sup>3,5</sup> their preferential adsorption on the numerous surface sites might lead to detachment from the metal center and leaching of the catalyst<sup>5</sup> or nanoparticle formation.<sup>3</sup> To preliminarily investigate this issue,  $(\text{Ph}_3\text{P})_2\text{Ni}(\text{CO})_2$  ( $3$ ) was applied to a silica surface from a solution of the complex in THF. After removal of the solvent, the material was heated to 50 °C in the dry state for three hours. The  $^{31}\text{P}$  MAS spectrum of the sample shows that a substantial amount of adsorbed  $\text{PPh}_3$  ( $1\text{a}$ ) is found on the surface besides  $3$  (Figure S13). It is noteworthy that the phosphine ligand becomes detached from the catalyst  $3$  in the absence of any substrate that could be an alternative reason for the dissociation of the phosphine ligand. This observation is in accordance with earlier results.<sup>5</sup> When performing the catalytic cyclotrimerization of phenylacetylene with an immobilized bisphosphine dicarbonylnickel complex, uncoordinated immobilized phosphine was found. This had been interpreted as substrate-induced leaching of the catalyst. However, the results presented here show that this leaching is not necessarily due to the competition of the substrate with the phosphine for a coordination site at the nickel center. The silica surface and adsorption of the phosphines can be the culprit. Furthermore, it should be mentioned that the temperature of 50 °C is moderate regarding the temperatures applied for real-life catalytic reactions. When  $(\text{Ph}_3\text{P})_2\text{Ni}(\text{CO})_2$  ( $3$ ) is heated to 50 °C together with silica in THF, only the signal of  $1\text{a}$  is visible in the  $^{31}\text{P}$  MAS spectrum after removal of the solvent (Figure S13). Therefore, it can be concluded that the silica surface efficiently removes the phosphine ligands from the nickel center, with the adsorption being the driving force. In contrast,  $3$  can be heated at 50 °C in the absence of silica in THF, a solvent with high coordinating potential, over three hours without any sign of decomposition (Figure S13).

## CONCLUSION

In this contribution we could, for the first time, demonstrate that solid  $\text{PPh}_3$  and  $\text{PCy}_3$  self-adsorb on silica surfaces in the absence of a solvent.  $^{31}\text{P}$  solid-state NMR spectroscopy was applied as a powerful multipronged technique to describe the adsorption process and behavior of the adsorbed species. The increased mobility of the adsorbed  $\text{PPh}_3$  molecules across the surface within the pores of silica manifests in shorter  $T_1$  relaxation times, different contact time characteristics, and reduced anisotropic interactions visible in the solid-state NMR spectra. Importantly, the transition between a monolayer occupancy on the surface and leftover polycrystalline materials is abrupt. Therefore, the formation of multiple layers on the surface can be excluded. The properties of the surface play a subordinate role in the adsorption process. Rigorously dried silica surfaces, exhibiting fewer silanol groups, lead to similar  $^{31}\text{P}$  CP/MAS chemical shifts and linewidths as "wet" silica surfaces with a high number of silanol groups. Even  $\text{Me}_3\text{Si}$ -modified silica does not change the adsorption characteristics of the phosphines. The mobilities of  $\text{PPh}_3$  molecules adsorbed on diverse silica surfaces could be further quantified by  $^2\text{H}$  solid-state NMR

measurements of the selectively deuterated versions PPh<sub>3</sub>-d<sub>1</sub>, PPh<sub>3</sub>-d<sub>3</sub>, and PPh<sub>3</sub>-d<sub>5</sub>. Finally, it could be demonstrated by stirring solutions of the complex (Ph<sub>3</sub>P)<sub>2</sub>Ni(CO)<sub>2</sub> with silica that the silica surface competes with the metal center for the phosphine ligands. Thus, the adsorption of phosphines on the silica surface plays a hitherto unrecognized role when immobilizing homogeneous catalysts on silica surfaces with phosphine linkers. The stripping of the complexes of their phosphine ligands might also open a pathway to generating single atom catalysts (SACs) in the future.<sup>44</sup>

## EXPERIMENTAL SECTION

**General Aspects and Silica.** All chemicals were purified by recrystallization prior to use. Solvents were distilled over Na and kept in Schlenk flasks under a purified nitrogen atmosphere. All procedures and syntheses were performed at a Schlenk line under inert atmosphere or in a glove-box unless mentioned otherwise. The silica gel was purchased from Merck with particle sizes of 0.2 to 0.063 mm, a specific surface area of 750 m<sup>2</sup>/g and average pore size of 40 Å and, where mentioned, 100 Å (400 m<sup>2</sup>/g). The silica was dried by oil pump vacuum at 600 °C for 6 days and stored under a nitrogen atmosphere. "Wet" silica was dried *in vacuo* at RT until no more water accumulated in a liquid nitrogen trap. Silica modified with Me<sub>3</sub>Si groups was prepared by suspending 150 g of RT-dried silica in 390 ml of distilled Me<sub>3</sub>SiOEt. The mixture was stirred at RT for 3 days, then the excess of Me<sub>3</sub>SiOEt was decanted and the modified silica was dried *in vacuo* at RT until no more liquids appeared in a cooling trap.

**NMR Measurements.** The <sup>2</sup>H and <sup>31</sup>P MAS and static NMR experiments were performed using a Bruker Avance 400 solid-state NMR spectrometer (Larmor frequencies 400 MHz for <sup>1</sup>H nuclei, 46.07 MHz for <sup>2</sup>H, 100.58 MHz for <sup>13</sup>C, and 161.49 MHz for <sup>31</sup>P) equipped with a two-channel 4 mm MAS NMR probe head. Glycine and adamantane have been used as external references for <sup>13</sup>C measurements and (NH<sub>4</sub>)<sub>2</sub>H<sub>2</sub>PO<sub>4</sub> for <sup>31</sup>P spectra. The standard single-pulse and cross-polarization sequences were applied for <sup>31</sup>P and <sup>2</sup>H nuclei, as described in the results and discussion section. The relaxation delays were 6 s for <sup>13</sup>C, 10 s for <sup>31</sup>P, and 60 s for <sup>2</sup>H solid-state NMR measurements. Typically, fewer than 1000 scans were sufficient for obtaining spectra of high quality, and no linebroadening had to be applied for processing.

The <sup>31</sup>P T<sub>1</sub> times were measured at a rotational frequency of 10 kHz using inversion–recovery (180°–τ–90°) experiments with well-calibrated RF-pulses, τ variations between 0.0001 and 8 s, and with a relaxation (recycle) delay of 10 s corresponding to complete relaxation of the nuclei after each pulse cycle. The experimental inversion–recovery curves (signal intensity versus τ time) have been treated with a standard nonlinear fitting computer program (LabPlot) based on the Levenberg–Marquardt algorithm.

The <sup>31</sup>P CSA parameters for PPh<sub>3</sub> and PCy<sub>3</sub> were obtained from the wideline spectra that were calculated based on the MAS spectra recorded at 2.5 kHz rotational speed using the dmfit software. The asymmetry parameters η for PPh<sub>3</sub> and PCy<sub>3</sub> were 0.00 and 0.65, respectively. The precision for the CSA values was ±1 ppm and for signal halfwidths ±10 Hz.

**Adsorption from Solution.** When the adsorption of phosphines on silica was carried out using a solution, the desired amount of phosphine, in the mg range as specified in the supplementary information, was added to ca. 30 ml of pentane or ether, which had been distilled from sodium/benzophenone and kept under nitrogen. This solution was then added to a 5.0 g portion of dried silica under a nitrogen atmosphere and stirred for 10 h. The pentane was then removed *in vacuo*. The non-volatile phosphines remained on the surface.

**Dry Adsorption.** The solid components **1** or **2** were ground together with silica with the indicated amounts manually for 1 h under an inert gas atmosphere. Subsequent monitoring is described in the results and discussion section.

**Surface Coverages of Adsorbed Species.** The table summarizes the amounts of adsorbed species per 1 g of rigorously dried silica and the corresponding number of adsorbed molecules on 100 nm<sup>2</sup> of silica surface. The surface coverages of **1a** were varied between 6.7 and 207 molecules per 100 nm<sup>2</sup> of silica surface (Figure S5), as discussed in the results section. A typical value for **1a** is given here.

Adsorbed	g per 1 g of silica	Molecules on 100 nm <sup>2</sup>
<b>1a</b>	0.613	206
<b>1a-d<sub>1</sub></b>	0.572	192
<b>1a-d<sub>3</sub></b>	0.362	120
<b>1a-d<sub>5</sub></b>	0.345	114
<b>2a</b>	0.101	32

**Syntheses of Deuterated Phosphines.** The selectively deuterated phosphines **1-d<sub>1</sub>**,<sup>45</sup> **1-d<sub>3</sub>**,<sup>45-48</sup> and **1-d<sub>5</sub>**<sup>49</sup> have been mentioned in classical publications, but detailed synthesis procedures were missing or based on the slow Grignard reactions starting from *p*-deuteriohalobenzenes, giving low yields. Only fragmentary analytical data could be reported at that time. Therefore, new syntheses, based on the use of <sup>n</sup>BuLi and starting from the inexpensive, commercially available *p*-dibromobenzene,<sup>50</sup> and full characterization are provided here and the <sup>2</sup>H NMR spectra are displayed in Figure S14.

**Synthesis of Diphenyl(*p*-bromophenyl)phosphine (1-Br<sub>1</sub>).** A 1.6 M solution of <sup>n</sup>BuLi in hexanes (13.75 ml, 22.0 mmol) was added dropwise to a stirred solution of 1,4-dibromobenzene (5.110 g, 21.66 mmol) in 50 ml of freshly distilled diethyl ether at –78 °C under a nitrogen atmosphere. The solution was slowly warmed up to room temperature and stirred for another 2 h. Then the transparent solution was cooled to –78 °C and chlorodiphenylphosphine (3.95 ml, 22.0 mmol) was added dropwise. The reaction mixture was stirred at room temperature over night and then filtered to remove LiCl. The solvent was removed *in vacuo*. The final product was recrystallized from acetone at –40 °C to yield 6.977 g (20.45 mmol, 94.4%) of **1-Br<sub>1</sub>** as a slightly yellow polycrystalline powder.

**<sup>1</sup>H NMR** (acetone-*d*<sub>6</sub>, 300.13 MHz)  $\delta$  = 7.56 (dd, <sup>3</sup>*J*<sub>H-H</sub> = 8.3 Hz, <sup>4</sup>*J*<sub>P-H</sub> = 0.9 Hz, 2 H, P(C<sub>6</sub>H<sub>4</sub>Br), PCCCCH), 7.41-7.38 (m, 6 H, PPh<sub>2</sub>, H<sub>m/p</sub>), 7.32-7.27 (m, 4 H, PPh<sub>2</sub>, H<sub>o</sub>), 7.20 (dd, <sup>3</sup>*J*<sub>H-H</sub> = 8.3 Hz, <sup>3</sup>*J*<sub>P-H</sub> = 6.8 Hz, 2 H, P(C<sub>6</sub>H<sub>4</sub>Br), PCCCH). **<sup>13</sup>C NMR** (acetone-*d*<sub>6</sub>, 75.47 MHz)  $\delta$  = 137.87 (d, <sup>1</sup>*J*<sub>P-C</sub> = 13.5 Hz, P(C<sub>6</sub>H<sub>4</sub>Br), PC), 136.01 (d, <sup>2</sup>*J*<sub>P-C</sub> = 20.2 Hz, P(C<sub>6</sub>H<sub>4</sub>Br), PCC), 132.43 (d, <sup>3</sup>*J*<sub>P-C</sub> = 6.8 Hz, P(C<sub>6</sub>H<sub>4</sub>Br), PCCC); 123.69 (s, CBr), 137.44 (d, <sup>1</sup>*J*<sub>P-C</sub> = 11.42 Hz, PPh<sub>2</sub>, C<sub>i</sub>), 134.31 (d, <sup>2</sup>*J*<sub>P-C</sub> = 19.9 Hz, PPh<sub>2</sub>, C<sub>o</sub>), 129.50 (d, <sup>3</sup>*J*<sub>P-C</sub> = 7.0 Hz, PPh<sub>2</sub>, C<sub>m</sub>), 129.85 (s, PPh<sub>2</sub>, C<sub>p</sub>). **<sup>31</sup>P NMR** (acetone-*d*<sub>6</sub>, 121.49 MHz)  $\delta$  = -6.21 (s). **MS (HR/EI<sup>+</sup>) M<sup>+</sup>** 339.9997 (100%, calcd. 340.0016, 100%), 341.9988 (97.0%, calcd. 341.9996, 97.3%).

**Synthesis of Diphenyl(*p*-deuterophenyl)phosphine (1-*d*<sub>1</sub>).** The Br/Li exchange was performed by adding 0.92 ml of a 1.6 M solution of <sup>n</sup>BuLi in hexane (1.50 mmol) dropwise to a stirred solution of **1-Br<sub>1</sub>** in ether at -78 °C. The solution was slowly warmed up to RT and stirred for another 2h. The clear solution was quenched with 10 ml of D<sub>2</sub>O and subsequently extracted with two 20 ml portions of ether. The organic phases were collected, dried over MgSO<sub>4</sub>, and concentrated to give a colorless solid. Further purification by recrystallization from acetone at -40 °C yielded 0.340 g (1.29 mmol, 88.4%) of **1-*d*<sub>1</sub>** as a colorless polycrystalline powder. mp 82-83 °C.

**<sup>1</sup>H NMR** (acetone-*d*<sub>6</sub>, 500.13 MHz)  $\delta$  = 7.38-7.36 (m, 8 H, DCCCH, PPh<sub>2</sub>, H<sub>m</sub>, H<sub>p</sub>), 7.30-7.29 (m, 6 H, DCCCH, PPh<sub>2</sub>, H<sub>o</sub>). **<sup>13</sup>C NMR** (acetone-*d*<sub>6</sub>, 125.76 MHz)  $\delta$  = 138.19 (d, <sup>1</sup>*J*<sub>P-C</sub> = 11.9 Hz, C<sub>i</sub>), 134.37 (d, <sup>2</sup>*J*<sub>P-C</sub> = 19.7 Hz, PPh<sub>2</sub>, C<sub>o</sub>), 129.32 (d, <sup>3</sup>*J*<sub>P-C</sub> = 6.9 Hz, DCC), 129.42 (d, <sup>3</sup>*J*<sub>P-C</sub> = 7.1 Hz, PPh<sub>2</sub>, C<sub>m</sub>), 129.67 (s, PPh<sub>2</sub>, C<sub>p</sub>). **<sup>31</sup>P NMR** (acetone-*d*<sub>6</sub>, 202.45 MHz)  $\delta$  = -5.93 (s). **<sup>2</sup>H NMR** (acetone-*d*<sub>6</sub>, 46.07 MHz)  $\delta$  = 7.98 (s). **MS (HR/EI<sup>+</sup>) M<sup>+</sup>** 263.1001 (100%, calcd. 263.0973, 100 %).

**Synthesis of Tri(*p*-bromophenyl)phosphine (1-Br<sub>3</sub>).** A solution of 1,4-dibromobenzene (4.509 g, 19.11 mmol) in 50 ml of ether was cooled to -78 °C. Then 11.95 ml of a 1.6 M solution of <sup>n</sup>BuLi in hexane (19.11 mmol) was added in a dropwise manner. The reaction mixture was allowed to warm up to RT slowly and stirred for 2 more hours. The clear solution was again cooled to -78 °C and PCl<sub>3</sub> (0.874 g, 6.38 mmol) was added dropwise. The reaction mixture was stirred at RT over night and then filtered to remove LiCl. The solvent was completely removed *in vacuo* and the product recrystallized from acetone. A slightly yellow-green polycrystalline powder of the product **1-Br<sub>3</sub>** was obtained (8.532 g, 17.10 mmol, yield 89.5%).

**<sup>1</sup>H NMR** (acetone-*d*<sub>6</sub>, 300.13 MHz)  $\delta$  = 7.61 (dd, <sup>3</sup>*J*<sub>H-H</sub> = 8.3 Hz, <sup>4</sup>*J*<sub>P-H</sub> = 1.2 Hz, 6 H, PCCCCH); 7.23 (dd, <sup>3</sup>*J*<sub>H-H</sub> = 8.3 Hz, <sup>3</sup>*J*<sub>P-H</sub> = 9.0 Hz, 6 H, PCCCH). **<sup>13</sup>C NMR** (acetone-*d*<sub>6</sub>, 75.47 MHz)  $\delta$  = 140.91 (d, <sup>1</sup>*J*<sub>P-C</sub> = 13.8 Hz, PC), 140.50 (d, <sup>2</sup>*J*<sub>P-C</sub> = 20.7 Hz, PCC), 137.15 (d, <sup>3</sup>*J*<sub>P-C</sub> = 7.1 Hz, PCCC), 128.69 (s, CBr). **<sup>31</sup>P NMR** (acetone-*d*<sub>6</sub>, 121.49 MHz)  $\delta$  = -8.10 (s). **MS (HR/EI<sup>+</sup>) M<sup>+</sup>** 497.7976 (100%, calcd. 497.8206, 100%).

**Synthesis of Tri(*p*-deuterophenyl)phosphine (1-*d*<sub>3</sub>).** <sup>n</sup>BuLi (2.52 ml of a 1.6 M solution in hexane, 4.04 mmol) was added dropwise to a stirred solution of tri(*p*-bromophenyl)phosphine (0.672 g, 1.35 mmol) in 50 ml of ether at -78 °C. The reaction mixture was allowed to warm to RT slowly, and then it was stirred for 2 more

hours. The clear solution was treated with 15 ml of D<sub>2</sub>O and subsequently extracted with two 20 ml portions of ether. The organic phases were combined and dried with MgSO<sub>4</sub>. Removal of the solvent *in vacuo* resulted in a white solid that was recrystallized from acetone. The product **1-*d*<sub>3</sub>** was obtained as colorless polycrystalline powder (0.305 g, 1.14 mmol, 84.5% yield). mp 81-82 °C.

**<sup>1</sup>H NMR** (acetone-*d*<sub>6</sub>, 500.13 MHz)  $\delta$  = 7.37 (d, <sup>3</sup>*J*<sub>H-H</sub> = 7.8 Hz, 6 H, PCCCCH), 7.29 (dd, <sup>3</sup>*J*<sub>H-H</sub> = 7.8 Hz, <sup>3</sup>*J*<sub>P-H</sub> = 8.0 Hz, 6 H, PCCCH). **<sup>13</sup>C NMR** (acetone-*d*<sub>6</sub>, 125.76 MHz)  $\delta$  = 138.19 (d, <sup>1</sup>*J*<sub>P-C</sub> = 11.6 Hz, PC), 134.37 (d, <sup>2</sup>*J*<sub>P-C</sub> = 19.8 Hz, PCC), 129.34 (d, <sup>3</sup>*J*<sub>P-C</sub> = 6.9 Hz, PCCC). **<sup>31</sup>P NMR** (acetone-*d*<sub>6</sub>, 202.45 MHz)  $\delta$  = -5.86 (s). **<sup>2</sup>H NMR** (acetone-*d*<sub>6</sub>, 46.07 MHz)  $\delta$  = 7.98 (s). **MS (HR/EI<sup>+</sup>) M<sup>+</sup>** 265.0664 (100 %, calcd. 265.1097, 100 %).

**Synthesis of Diphenyl(pentadeuterophenyl)phosphine (1-*d*<sub>5</sub>).** A solution of bromobenzene-*d*<sub>5</sub> (1.50 ml, 14.25 mmol) in 50 ml of ether was cooled to -78 °C. Under stirring 8.9 ml of a 1.6 M solution of <sup>n</sup>BuLi in hexane (14.25 mmol) was added in a dropwise manner. The solution was allowed to warm up slowly to RT and then stirred for another 2 h. The clear solution was cooled to -78 °C and ClPPh<sub>2</sub> (2.56 ml, 14.25 mmol) was added dropwise. The reaction mixture was stirred at RT over night and then filtered to remove LiCl. The solvent was removed *in vacuo* and the product **1-*d*<sub>5</sub>** recrystallized from acetone, which yielded 3.055g (11.42 mmol, 80.1%) of a colorless polycrystalline powder. mp 83-84 °C.

**<sup>1</sup>H NMR** (acetone-*d*<sub>6</sub>, 500.13 MHz)  $\delta$  = 7.39-7.37 (m, 6 H, H-7/H-8); 7.30-7.27 (m, 4 H, H-6). **<sup>13</sup>C NMR** (acetone-*d*<sub>6</sub>, 125.76 MHz)  $\delta$  = 138.22 (d, <sup>1</sup>*J*<sub>P-C</sub> = 11.6 Hz, C<sub>i</sub>), 134.38 (d, <sup>2</sup>*J*<sub>P-C</sub> = 19.7 Hz, C<sub>o</sub>), 129.45 (d, <sup>3</sup>*J*<sub>P-C</sub> = 6.8 Hz, C<sub>m</sub>), 129.68 (s, C<sub>p</sub>). **<sup>31</sup>P NMR** (acetone-*d*<sub>6</sub>, 202.45 MHz)  $\delta$  = -6.17 (s). **<sup>2</sup>H NMR** (acetone-*d*<sub>6</sub>, 46.07 MHz)  $\delta$  = 7.98 (s, <sup>2</sup>H<sub>m/p</sub>), 7.89 (s, <sup>2</sup>H<sub>o</sub>). **MS (HR/EI<sup>+</sup>) M<sup>+</sup>** 267.1054 (100%, calcd. 267.1220, 100%).

**Heating (Ph<sub>3</sub>P)<sub>2</sub>Ni(CO)<sub>2</sub> (3) in solvent.** (Ph<sub>3</sub>P)<sub>2</sub>Ni(CO)<sub>2</sub> (**3**) (52.3 mg, 0.0818 mmol) was dissolved in 10 ml of THF. The solution was heated for 3 h at 50 °C and after cooling was measured by <sup>31</sup>P NMR. The spectrum showed only the signal of **3** at 35 ppm.

**Heating 3 in THF in the presence of silica.** (Ph<sub>3</sub>P)<sub>2</sub>Ni(CO)<sub>2</sub> (**3**) (12 mg, 0.018 mmol) was mixed with 1.3 g of silica. After adding 10 ml of THF the mixture was stirred at 50 °C for 3h. Then the solvent was removed *in vacuo* and the resulting material was measured with <sup>31</sup>P MAS. Only the signal of adsorbed PPh<sub>3</sub> (**1a**) was visible.

**Dry heating of 3 on silica.** Silica (1.1 g) was added to a solution of (Ph<sub>3</sub>P)<sub>2</sub>Ni(CO)<sub>2</sub> (**3**) (52.3 mg, 0.0818 mmol) in 10 ml of THF. The mixture was stirred for 20 min before the solvent was removed *in vacuo*. Then the dry material was stirred at 50 °C for 3h and after cooling its <sup>31</sup>P MAS spectrum was recorded. It showed the signals of residual complex **3** (32 ppm) and adsorbed PPh<sub>3</sub> (-6 ppm) (Figure S13).

## ASSOCIATED CONTENT

### Supporting information

Supporting Information is available free of charge at <https://pubs.acs.org/doi/>

Additional  $^{31}\text{P}$  and  $^2\text{H}$  solid-state and solution NMR spectra, surface coverages, linewidths, contact time characteristics and  $T_1$  relaxation times.

## AUTHOR INFORMATION

### Corresponding Authors

**Dr. Janet Blümel** – Department of Chemistry, Texas A&M University, College Station, TX, 77842-3012, USA; <https://orcid.org/0000-0002-6557-3518>; email: [bluemel@tamu.edu](mailto:bluemel@tamu.edu)

**Dr. Yuan Yang** – Department of Chemistry, Colorado School of Mines, Golden, CO, USA  
email: [yuanyang@mines.edu](mailto:yuanyang@mines.edu)

### Author

John C. Hoefler – Department of Chemistry, Texas A&M University, College Station, TX, 77842-3012, USA; <https://orcid.org/0000-0002-6684-8683>.

### Author Contributions

The manuscript was written through contributions of all authors. The project management and design was led by J.B. and Y.Y. The syntheses and NMR experiments were performed by J.C.H. and Y.Y. All authors have given approval to the final version of the manuscript.

### Notes

The authors declare no competing financial interests.

## ACKNOWLEDGMENTS

This work was supported by the National Science Foundation (CHE-1900100).

## REFERENCES

- (1) Callister Jr., W. D. *Materials Science and Engineering: An Introduction (7th ed.)*; John Wiley & Sons: New York, **2006**.
- (2) Shakeri, E.; Blümel, J. Creating Well-Defined Monolayers of Phosphine Linkers Incorporating Ethoxysilane Groups on Silica Surfaces for Superior Immobilized Catalysts. *Appl. Surf. Sci.* **2023**, *615*, 156380.
- (3) Guenther, J.; Reibenspies, J.; Blümel, J. Synthesis and Characterization of Tridentate Phosphine Ligands Incorporating Ethoxysilane Groups and Long Alkyl Chains for Immobilizing Molecular Rhodium Catalysts. *Mol. Catal.* **2019**, *479*, 110629.
- (4) Reinhard, S.; Soba, P.; Rominger, F.; Blümel, J. New Silica-Immobilized Nickel Catalysts for Cyclotrimerizations of Acetylenes. *Adv. Synth. Catal.* **2003**, *345*, 589-602.
- (5) Reinhard, S.; Behringer, K. D.; Blümel, J. Immobilized Nickel Catalysts for Cyclotrimerizations of Acetylenes: Enhancement of Activities, Stabilities, and Lifetimes. *New J. Chem.* **2003**, *27*, 776-778.
- (6) Scott, R. P. W. *Silica Gel and Bonded Phases*, John Wiley and Sons, New York, 1993.
- (7) Cluff, K. J.; Schnellbach, M.; Hilliard, C. R.; Blümel, J. The adsorption of chromocene and ferrocene on silica: A solid-state NMR study. *J. Organomet. Chem.* **2013**, *744*, 119-124.
- (8) Cluff, K. J.; Blümel, J. Adsorption of Metallocenes on Silica. *Chem. Eur. J.* **2016**, *22*, 16562-16575.
- (9) Cluff, K. J.; Bhuvanesh, N.; Blümel, J. Adsorption of Ruthenium and Iron Metallocenes on Silica: A Solid-State NMR Study. *Organometallics* **2014**, *33*, 2671-2680.
- (10) Benzie, J. W.; Harmon-Welch, G. E.; Hoefler, J. C.; Bakhmutov, V. I.; Blümel, J. Molecular Dynamics and Surface Interactions of Nickelocene Adsorbed on Silica: A Paramagnetic Solid-State NMR Study. *Langmuir* **2022**, *38*, 7422-7432.

(11) Kharel, S.; Cluff, K. J.; Bhuvanesh, N.; Gladysz, J. A.; Blümel, J. Structures and Dynamics of Secondary and Tertiary Alkylphosphine Oxides Adsorbed on Silica. *Chem. Asian J.* **2019**, *14*, 2704-2711.

(12) Hilliard, C. R.; Kharel, S.; Cluff, K. J.; Bhuvanesh, N.; Gladysz, J. A.; Blümel, J. Structures and Unexpected Dynamic Properties of Phosphine Oxides Adsorbed on Silica Surfaces. *Chem. Eur. J.* **2014**, *20*, 17292-17295.

(13) Cluff, K. J.; Blümel, J. Adsorption of ferrocene on carbon nanotubes, graphene, and activated carbon. *Organometallics* **2016**, *35*, 3939-3948.

(14) Hubbard, P. J.; Benzie, J. W.; Bakhmutov, V. I.; Janet Blümel, J., Ferrocene adsorbed on silica and activated carbon surfaces: a solid-state NMR study of molecular dynamics and surface interactions. *Organometallics* **2020**, *39*, 1080-1091.

(15) Hubbard, P. J.; Benzie, J. W.; Bakhmutov, V. I.; Blümel, J. Disentangling Different Modes of Mobility for Triphenylphosphine Oxide Adsorbed on alumina. *J. Chem. Phys.* **2020**, *152*, 054718.

(16) Günther, H.; Oepen, S.; Ebener, M.; Francke, V. *Magn. Reson. Chem.* **1999**, *37*, S142-S146.

(17) Oprunenko, Y.; Gloriov, I.; Lyssenko, K.; Malyugina, S.; Mityuk, D.; Mstislavsky, V.; Günther, H.; von Firks, G.; Ebener, M. Chromium tricarbonyl complexes with biphenylene as  $\eta^6$  ligand: synthesis, structure, dynamic behaviour in solid state and thermal  $\eta^6, \eta^6$ -haptotropic rearrangements. Experimental (NMR) and theoretical (DFT) studies. *J. Organomet. Chem.* **2002**, *656*, 27-42.

(18) Shenderovich, I. G. For Whom a Puddle Is the Sea? Adsorption of Organic Guests on Hydrated MCM-41 Silica. *Langmuir* **2020**, *36*, 11383-11392.

(19) Bakhmutov, V. I.; Strategies for solid-state NMR studies of materials: from diamagnetic to paramagnetic porous solids. *Chem. Rev.* **2011**, *111*, 530-562.

(20) Shenderovich, I. G.; Limbach H.-H. Solid State NMR for Nonexperts: An Overview of Simple but General Practical Methods. *Solids* **2021**, *2*, 139-154.

(21) Duncan, T. M. *A Compilation of Chemical Shift Anisotropies*. Farragut Press: Chicago, IL, 1990.

(22) Schmidt-Rohr, K.; Spiess, H. W. *Multidimensional Solid-State NMR and Polymers*. Academic Press: London, UK, 1994.

(23) Samudrala, K. K.; Huynh, W.; Dorn, R. W.; Rossini, A. J.; Conley, M. P. Formation of a Strong Heterogeneous Aluminum Lewis Acid on Silica. *Angew. Chem. Int. Ed.* **2022**, *61*, e202205745.

(24) Carnahan, S. L.; Chen, Y.; Wishart, J. F.; Lubach, J. W.; Rossini, A. J. Magic angle spinning dynamic nuclear polarization solid-state NMR spectroscopy of  $\gamma$ -irradiated molecular organic solids. *Solid State Nucl. Magn. Reson.* **2022**, *119*, 101785.

(25) Rossi, L. M.; Fiorio, J. L.; Garcia, M. A. S.; Ferraz, C. P. The Role and Fate of Capping Ligands in Colloidally Prepared Metal Nanoparticle Catalysts. *Dalton Trans.* **2018**, *47*, 5889-5915.

(26) Weston, M. H.; Morris, W.; Siu, P. W.; Hoover, W. J.; Cho, D.; Richardson, R. K.; Farha, O. K. Phosphine Gas Adsorption in a Series of Metal-Organic Frameworks. *Inorg. Chem.* **2015**, *54*, 8162-8164.

(27) Wyrick, J.; Wang, X.; Nambodiri, P.; Kashid, R. V.; Fei, F.; Fox, J.; Silver, R. Enhanced Atomic Precision Fabrication by Adsorption of Phosphine into Engineered Dangling Bonds on H-Si Using STM and DFT. *ACS Nano* **2022**, *16*, 19114-19123.

(28) Pavlova, T. V.; Zhidomirov, G. M.; Eltsov, K. N. First-Principle Study of Phosphine Adsorption on Si(001)-2  $\times$  1-Cl. *J. Phys. Chem. C* **2018**, *122*, 1741-1745.

(29) Sgarbossa, F.; Levarato, A.; Carturan, S. M.; Rizzi, G. A.; Tubaro, C.; Ciatto, G.; Bondino, F.; Piš, I.; Napolitani, E.; De Salvador, D. Phosphorus Precursors Reactivity versus Hydrogenated Ge Surface: Towards a Reliable Self-Limited Monolayer Doping. *Appl. Surf. Sci.* **2021**, *541*, 148532.

(30) Rodrigues, J.; Culver, D. B.; Conley, M. P. Generation of Phosphonium Sites on Sulfated Zirconium Oxide: Relationship to Brønsted Acid Strength of Surface -OH Sites. *J. Am. Chem. Soc.* **2019**, *141*, 1484-1488.

(31) Blümel, J. Reactions of Phosphines with Silica: A Solid-state NMR Study. *Inorg. Chem.* **1994**, *33*, 5050-5056.

(32) Sharma, R.; Holland, G. P.; Solomon, V. C.; Zimmermann, H.; Schifffenhaus, S.; Amin, S. A.; Buttry, D. A.; Yarger, J. L. NMR Characterization of Ligand Binding and Exchange Dynamics in Triphenylphosphine-Capped Gold Nanoparticles. *J. Phys. Chem. C* **2009**, *113*, 16387-16393.

- (33) Blümel, J. Reactions of Ethoxysilanes with Silica: A Solid-State NMR Study. *J. Am. Chem. Soc.* **1995**, *117*, 2112-2113.
- (34) Sommer, J.; Yang, Y.; Rambow, D.; Blümel, J. Immobilization of Phosphines on Silica: Identification of Byproducts via <sup>31</sup>P CP/MAS Studies of Model Alkyl-, Aryl-, and Ethoxyphosphonium Salts. *Inorg. Chem.* **2004**, *43*, 7561-7563.
- (35) Ziemer, B.; Rabis, A.; Steinberger, H.-U. Triclinic Polymorphs of Triphenylphosphine and Triphenylphosphine Sulfide. *Acta Cryst. C: Crystal Struct. Commun.* **2000**, *56*, e58.
- (36) Gedat, E.; Schreiber, A.; Albrecht, J.; Emmler, Th.; Shenderovich, I.; Findenegg, G. H.; Limbach, H.-H.; Buntkowsky, G. <sup>2</sup>H-Solid-State NMR Study of Benzene-*d*<sub>6</sub> Confined in Mesoporous Silica SBA-15. *J. Phys. Chem. B* **2002**, *106*, 1977-1984.
- (37) Benzie, J. W.; Bakhmutov, V. I.; Blümel, J. Benzene Adsorbed on Activated Carbon: A Comprehensive Solid-State NMR Study of Interactions with the Pore Surface and Molecular Motions. *J. Phys. Chem. C* **2020**, *124*, 21532-21537.
- (38) Harmon-Welch, G. E.; Hoefler, J. C.; Trujillo, M. R.; Bhuvanesh, N.; Bakhmutov, V. I.; Blümel, J. Creating Solid Solutions of Metallocenes: Migration of Nickelocene into the Ferrocene Crystal Lattice in the Absence of a Solvent. *J. Phys. Chem. C* **2023**, *127*, 3059-3066.
- (39) Reinhard, S.; Blümel, J. <sup>31</sup>P CP/MAS NMR of Polycrystalline and Immobilized Phosphines and Catalysts with fast Sample Spinning. *Magn. Reson. Chem.* **2003**, *41*, 406-416.
- (40) Blümel, J.; Hiller, W.; Herker, M.; Köhler, F. H. Solid-State Paramagnetic NMR Spectroscopy of Chromocenes. *Organometallics* **1996**, *15*, 3474-3476.
- (41) Xiong, J.; Lock, H.; Chuang, I. S.; Keeler, C.; Maciel, G. E. *Environ. Sci. Technol.* **1999**, *33*, 2224-2233.
- (42) Hoefler, J. C.; Vu, A.; Perez, A. J.; Blümel, J. Immobilized Di(hydroperoxy)propane Adducts of Phosphine Oxides as Traceless and Recyclable Oxidizing Agents. *Appl. Surf. Sci.* **2023**, *629*, 157333.
- (43) Blümel, J. Reactions of Ethoxysilanes with Silica: A Solid-State NMR Study. *J. Am. Chem. Soc.* **1995**, *117*, 2112-2113.
- (44) Ding, K.; Cullen, D. A.; Zhang, L.; Cao, Z.; Roy, A. D.; Ivanov, L. N.; Cao, D. A general synthesis approach for supported bimetallic nanoparticles via surface inorganometallic chemistry. *Science* **2018**, *362*, 560-564.
- (45) Yakovleva, E. A.; Tsvetkov, E. N.; Lobanov, D. I.; Shatenshtein, A. I.; Kabachnik, M. I. Protophilic Deuteroexchange of Certain Tertiary Arylphosphines and Their Oxides. *Tetrahedron* **1969**, *25*, 1165-1173.
- (46) Benassi, R.; Schenetti, M. L.; Taddei, F.; Vivarelli, P.; Dembech, P. <sup>1</sup>H Nuclear Magnetic Resonance Study of Para-Substituted Derivatives of Triphenylphosphine. *J. Chem. Soc. Perkin Trans. 2* **1974**, *2*, 1338-1342.
- (47) Morita, D. K.; Stille, J. K.; Norton, J. R. Methyl/Phenyl Exchange between Palladium and a Phosphine Ligand. Consequences for Catalytic Coupling Reactions. *J. Am. Chem. Soc.* **1995**, *117*, 8576-8581.
- (48) Baldwin, R. A.; Cheng, M. T. Arylenebis(tertiary phosphines) and - (phosphinic acids). *J. Org. Chem.* **1966**, *32*, 1572-1577.
- (49) Fukuda, K.; Iwasawa, N.; Takaya, J. Ruthenium-Catalyzed Ortho C-H Borylation of Arylphosphines. *Angew. Chemie - Int. Ed.* **2019**, *58*, 2850-2853.
- (50) Baker, J. H.; Bhuvanesh, N.; Blümel, J. Tetrakisphosphines with tetra(biphenyl)silane and -stannane cores as rigid scaffold linkers for immobilized catalysts. *J. Organomet. Chem.* **2017**, *847*, 193-203.

1  
2  
3  
4  
5  
6  
7  
8  
9  
10  
11  
12  
13  
14  
15  
16  
17  
18  
19  
20  
21  
22  
23  
24  
25  
26  
27  
28  
29  
30  
31  
32  
33  
34  
35  
36  
37  
38  
39  
40  
41  
42  
43  
44  
45  
46  
47  
48  
49  
50  
51  
52  
53  
54  
55  
56  
57  
58  
59  
60